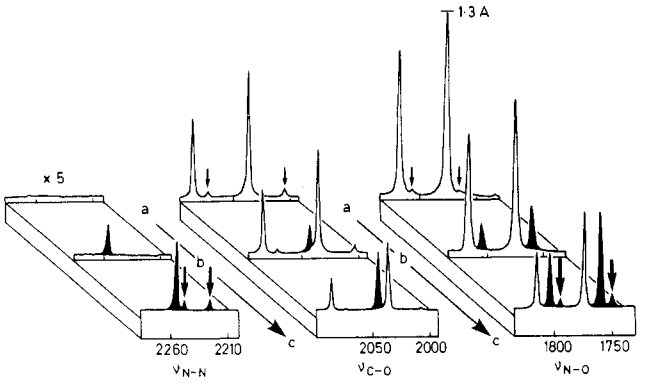

Figure 1. IR spectra of $Fe(CO)_2(NO)_2$ and photoproducts in liquid Kr doped with 2% N_2 at −155 °C. The spectra are plotted in absorbance, and the N–N region is expanded ×5: (a) prior to photolysis, arrowed peaks due to natural-abundance ^{13}C and ^{15}N (see table); (b) after 4-min UV photolysis, black bands due to $Fe(CO)(N_2)(NO)_2$; (c) after a further 66-min photolysis, arrowed bands due to $Fe(N_2)_2(NO)_2$.

stretching region and two strong bands in both the C–O and N–O stretching regions, at wavenumbers close to those of matrix-isolated $Fe(CO)_2(NO)_2$ but without the matrix splittings (see Table I). There are also four weak bands (arrowed) due to naturally occurring ^{13}C (1.1%) and ^{15}N (0.35%). Table I gives the force constants calculated for a simple energy-factored force field, which ignores any coupling between C–O and N–O vibrations. The good agreement between experimental and calculated frequencies confirms this apparent independence of the CO and NO vibrators. After 4 min of UV photolysis (spectrum b), the bands due to $Fe(CO)_2(NO)_2$ have decreased, and one new band has appeared in the ν_{N-N} region, one has appeared in the ν_{C-O} region, and two new bands have appeared in the ν_{N-O} region. These bands, colored black in spectrum b, are close in frequency to those of matrix-isolated[4] $Fe(CO)(N_2)(NO)_2$ and can be assigned unambiguously to this molecule (see Table I).

Further UV photolysis (spectrum c) decreases the concentration of $Fe(CO)_2(NO)_2$, increases the concentration of the primary photoproduct $Fe(CO)(N_2)(NO)_2$, and generates a third species with two N–N bands, no C–O bands, and two N–O bands (arrowed). These bands are clearly due to $Fe(N_2)_2(NO)_2$ and are compared in the table with the matrix data.[4] There was difficulty in detecting any N–N stretching bands for this molecule in the matrix[4] because they were weak, and this may explain the larger difference in frequency for these bands between liquid Kr solution and matrix. Thus, our experiments show that UV photolyis of $Fe(CO)_2(NO)_2$ in liquid Kr leads to stepwise substitution of the CO groups, just as it did in the matrix.[4]

$Ni(CO)_3N_2$, generated by photolysis of $Ni(CO)_4$ in liquefied Kr/N_2, reacts rapidly[2] with CO ($t_{1/2} \sim {}^1/_2$ min at −155 °C). At the same temperature $Fe(N_2)_2(NO)_2$ disappears ($t_{1/2} \sim$ 40 min), presumably to form $Fe(CO)(N_2)(NO)_2$, although unfortunately the expected growth in the bands of $Fe(CO)(N_2)(NO)_2$ could not be established with certainty in our experiment. Even allowing for the difference in CO concentrations between the Ni and Fe experiments, it is clear that, at −155 °C, $Fe(N_2)_2(NO)_2$ is considerably less reactive toward CO than $Ni(CO)_3(N_2)$.

By contrast, the primary photoproduct $Fe(N_2)(CO)(NO)_2$ is almost completely stable at −155 °C and only begins to disappear as the temperature of the solution is raised. Warming the solution from −155 to −107 °C over 2 h led to a ~50% decrease in the intensity of the $Fe(CO)(N_2)(NO)_2$ bands with a corresponding increase in the bands due to $Fe(CO)_2(NO)_2$ confirming that reaction 1 is occurring. Thus, $Fe(CO)(N_2)(NO)_2$ is very much less reactive toward CO than is $Ni(CO)_3(N_2)$, which is not surprising.[3]

$$Fe(CO)(N_2)(NO)_2 + CO \rightarrow Fe(CO)_2(NO)_2 + N_2 \quad (1)$$

This experiment again demonstrates the value of liquefied noble-gas solvents. We can now establish the thermal stabilities of unstable molecules, previously only observed in solid matrices at very low temperatures, and the thermal chemistry of a whole new class of compounds is accessible.

Experimental Section

The high-pressure/low-temperature IR cell (2.7-cm path length; 8.5-mL volume) has been described previously.[1,2] Krypton and N_2 (BOC research grade) were used without further purification. $Fe(CO)_2(NO)_2$ was prepared by published methods.[6] All spectra were recorded with a Nicolet MX-3600 FTIR interferometer using 32K data points (0.7-cm^{-1} resolution), 3 degrees of zero filling, and Happ–Genzel Apodization in the Fourier transform, and 100 scans were performed for each data collection. The UV photolysis source was Phillips 25-W Cd lamp.

Acknowledgment. We are grateful to Dr. W. B. Maier, Dr. M. B. Simpson, and J. G. McLaughlin for advice and to the SERC for support.

Registry No. $Fe(CO)_2(NO)_2$, 13682-74-1; $Fe(CO)(N_2)(NO)_2$, 63576-04-5; $Fe(N_2)_2(NO)_2$, 63576-05-6; Kr, 7439-90-9; N_2, 7727-37-9.

(6) See e.g.: "Organometallic Synthesis"; Eisch, J. J., King, R. B., Eds.; Academic Press: London, 1965; Vol. 1.
(7) Perutz, R. N.; Turner, J. J. *Inorg. Chem.* **1975**, *14*, 262.

Contribution from the Molecular Structure Center and the Department of Chemistry, Indiana University, Bloomington, Indiana 47405

Reactivity of a Bridging Sulfhydryl Ligand, S-Alkylation of $[Mo(NC_6H_4CH_3)(S_2P(OC_2H_5)_2)]_2(\mu\text{-}S)(\mu\text{-}SH)(\mu\text{-}O_2CCF_3)$, and Structure of $[Mo(NC_6H_4CH_3)(S_2P(OC_2H_5)_2)]_2(\mu\text{-}S)(\mu\text{-}SCH_3)(\mu\text{-}O_2CCF_3)$

Mark E. Noble, Kirsten Folting, J. C. Huffman,* and R. A. D. Wentworth*

Received May 11, 1983

An increased attention to ligated sulfhydryl groups may be traced in part to an awakening interest in hydrodesulfurization (HDS) during the refinement of petroleum. The appearance of this ligand on the surface of a laboratory catalyst for HDS after the chemisorption of molecular hydrogen suggests that the ligand is also formed during HDS over the similar commercial catalyst.[1]

Nucleophilic properties resembling those of a thiol appear to be characteristic of terminal and most bridging sulfhydryl ligands. For example, the bridging ligands in $[Fe(CO)_3(\mu\text{-}SH)]_2$ can be alkylated with either alkyl halides or activated alkenes.[2] The properties of the bridging sulfhydryl ligands in $[(\eta^5\text{-}C_5H_4CH_3)Mo(\mu\text{-}S)(\mu\text{-}SH)]_2$, however, appear to be unique. Unlike a thiol, this compound reacts with ethylene and does so with the formation of two bridging 1,2-dithiolates and the elimination of H_2.[3] The relatively high formal oxi-

(1) The chemisorption of molecular hydrogen by MoS_2 results in ligated SH groups as shown by: Badger, E. H. M.; Friggith, R. H.; Newling, W. S. B. *Proc. R. Soc. London Ser. A* **1949**, *197*, 184. The catalytic properties of MoS_2 during hydrodesulfurization have been likened to those of the industrial catalyst by: Kolberg, S.; Amberg, C. H. *Can. J. Chem.* **1966**, *44*, 2623.
(2) Seyferth, D.; Henderson, R. S. *J. Organomet. Chem.* **1981**, *218*, C34.
(3) Rakowski DuBois, M.; Van Derveer, M. C.; DuBois, D. L.; Haltiwanger, R. C.; Miller, W. K. *J. Am. Chem. Soc.* **1980**, *102*, 7456.

0020-1669/84/1323-0631$01.50/0

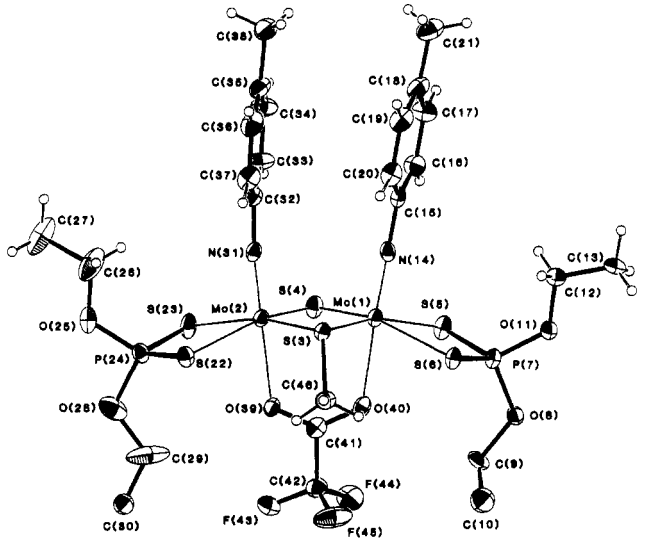

Figure 1. An ORETP drawing of $[Mo(NC_6H_4CH_3)(S_2P(OC_2H_5)_2)]_2(\mu\text{-}S)(\mu\text{-}SCH_3)(\mu\text{-}O_2CCF_3)$.

Table I. Selected Bond Distances (Å) and Angles (deg)

Mo(1)-Mo(2)	2.844 (1)	Mo(2)-S(3)	2.437 (1)
Mo(1)-S(3)	2.437 (2)	Mo(2)-S(4)	2.353 (2)
Mo(1)-S(4)	2.349 (2)	Mo(2)-S(22)	2.548 (2)
Mo(1)-S(5)	2.518 (2)	Mo(2)-S(23)	2.493 (2)
Mo(1)-S(6)	2.526 (1)	Mo(2)-N(31)	1.729 (5)
Mo(1)-N(14)	1.722 (5)	Mo(2)-O(39)	2.272 (4)
Mo(1)-O(40)	2.275 (4)	S(3)-C(46)	1.817 (6)
S(3)-Mo(1)-S(4)	107.1 (1)	Mo(1)-N(14)-C(15)	176.4 (4)
S(3)-Mo(2)-S(4)	107.0 (1)	Mo(2)-N(31)-C(32)	172.2 (4)
Mo(1)-S(3)-Mo(2)	71.4 (0)	Mo(1)-S(3)-C(46)	112.8 (2)
Mo(1)-S(4)-Mo(2)	74.4 (0)	Mo(2)-S(3)-C(46)	114.6 (2)
S(5)-Mo(1)-S(6)	78.5 (0)	S(4)-S(3)-C(46)	161.4 (2)
S(22)-Mo(2)-S(23)	78.7 (0)		

dation states of the metal atoms in this compound and the presence of both sulfur and sulfhydryl ligands in the bridge may be responsible for the unusual behavior.

These characteristics are also found in $[Mo(NC_6H_4CH_3)(S_2P(OC_2H_5)_2)]_2(\mu\text{-}S)(\mu\text{-}SH)(\mu\text{-}O_2CCF_3)$, a compound that can be prepared from the reaction of $[Mo(NC_6H_4CH_3)(\mu_3\text{-}S)(S_2P(OC_2H_5)_2)]_4$ and CF_3CO_2H.[4] In this paper, we establish a method for alkylation of the new sulfhydryl compound, examine the mechanistic implications of that method, and demonstrate the molecular structure of $[Mo(NC_6H_4CH_3)(S_2P(OC_2H_5)_2)]_2(\mu\text{-}S)(\mu\text{-}SCH_3)(\mu\text{-}O_2CCF_3)$.

Results and Discussion

The study began by an examination of the possible alkylation of $[Mo(NC_6H_4CH_3)(\mu_3\text{-}S)(S_2P(OC_2H_5)_2)]_4$ (**T**), but after the addition of CH_3Br, no reaction was observed during 24 h at ambient temperature in either CH_2Cl_2 or benzene. A very slow reaction ensued, however, after the addition of 2 equiv of CF_3CO_2H. The rate of the reaction was increased by the addition of $(C_2H_5)_3N$, and still more favorable kinetics were realized after the addition of the salt, $[(C_2H_5)_3NH]O_2CCF_3$. This pattern is explicable in terms of the reactions shown in eq 1–4, wherein $D\cdot H,CF_3CO_2$ is $[Mo(NC_6H_4CH_3)(S_2P(OC_2H_5)_2)]_2(\mu\text{-}S)(\mu\text{-}SH)(\mu\text{-}O_2CCF_3)$ and

$$\mathbf{T} + 2CF_3CO_2H \rightleftarrows 2D\cdot H,CF_3CO_2 \quad (1)$$

$$D\cdot H,CF_3CO_2 + (C_2H_5)_3N \rightarrow D\cdot CF_3CO_2^- + (C_2H_5)_3NH^+ \quad (2)$$

$$2D\cdot CF_3CO_2^- \rightleftarrows \mathbf{T} + 2CF_3CO_2^- \quad (3)$$

$$D\cdot CF_3CO_2^- + CH_3Br \rightarrow D\cdot CH_3,CF_3CO_2 + Br^- \quad (4)$$

Table II. Comparison of Some Molecular[a,b] Parameters of $D\cdot CH_3,CF_3CO_2$ and $D\cdot H,CF_3CO_2$

	$D\cdot CH_3$, CF_3CO_2	$D\cdot H$, CF_3CO_2
Mo-Mo, Å	2.844 (1)	2.839 (2)
Mo-S_b, Å	2.351 (3)	2.348 (9)
Mo-S(CH_3 or H), Å	2.437 (0)	2.44 (1)
Mo-S_l(trans to S_b), Å	2.54 (2)	2.540 (4)
Mo-S_l(trans to S(CH_3 or H)), Å	2.51 (2)	2.509 (4)
Mo-N, Å	1.726 (5)	1.74 (1)
Mo-O, Å	2.274 (2)	2.26 (0)
Mo-S_b-Mo, deg	74.4 (0)	74.4 (1)
Mo-S(CH_3 or H)-Mo, deg	71.4 (0)	71.1 (1)
S_b-Mo-S(CH_3 or H), deg	107.1 (1)	107.3 (6)
S_l-Mo-S_l, deg	78.6 (1)	78.4 (3)
Mo-N-C, deg	174 (3)	174 (2)
S_b-S_b-X (X = C(46) or H), deg	119.0 (2)	107 (8)
sum of angles around C(41), deg[c]	359.5 (9)	361 (3)

[a] Averages are given where required. [b] S_b = bridging sulfur atom, and S_l = sulfur atom from a dithiophosphate ligand. [c] This parameter indicates the planarity of the carboxylate ligand.

$D\cdot CF_3CO_2^-$ is the corresponding conjugate base. The reactions in eq 1–3 have been discussed previously.[4] When benzene was used to allow the separation of insoluble $[(C_2H_5)_3NH]Br$, orange crystalline $D\cdot CH_3,CF_3CO_2$ was obtained in 87% yield after recrystallization. The method also afforded the orange ethyl and benzyl derivatives in excellent purity and yields when CH_3Br was replaced by ethyl and benzyl bromides, respectively.

These results are completely consistent with S-alkylation and a relationship between $D\cdot H,CF_3CO_2$ and $D\cdot CF_3CO_2^-$, which resembles the one between a thiol and a thiolate. Nevertheless, a demonstration of S-alkylation is required since N-alkylation of a bound arylimido ligand with CH_3Br has been found previously.[5]

The ^1H and ^{31}P NMR spectra (220 and 40.5 MHz, respectively) of $D\cdot CH_3,CF_3CO_2$ in $CDCl_3$ consist of doubled signals that coalesce on raising the temperature and return when the temperature is decreased. An equilibrium between $D\cdot CH_3,CF_3CO_2$ and $D\cdot CH_3^+$ is not responsible since the pattern is unaltered by the addition of $[(C_2H_5)_3NH]O_2CCF_3$. The ^{31}P NMR spectra indicated that the ratio of the intensities of the two signals was about 5.6 at about 20 °C while coalescence occurred at about 53 °C. Both above and below coalescence, the ^1H and ^{31}P NMR spectra provided proof that both arylimido ligands as well as both dithiophosphate ligands are equivalent. The doubled signals are then ascribed to conformational isomers arising from inversion at the sulfur atom of a bridging methanethiolate ligand. Similar isomerism has been reported for bridging alkanethiolate ligands in other compounds[6] and for the sulfhydryl ligand in $D\cdot H,CF_3CO_2$.[4]

An X-ray study provided final proof of S-methylation as shown by the ORTEP drawing of $[Mo(NC_6H_4CH_3)(S_2P(OC_2H_5)_2)]_2(\mu\text{-}S)(\mu\text{-}SCH_3)(\mu\text{-}O_2CCF_3)$ in Figure 1. Although disorder was observed at C(10) and C(30), it was resolved after two sites with occupancy factors of 0.5 were located in each case. All hydrogen atoms except for those in the vicinity of the disorder were located. No unusual distances or angles were found around the periphery of the MoS_2Mo core. Selected bond distances and angles were given in Table I while Table II presents a comparison of some of the remarkable similarities in and around the MoS_2Mo cores of $D\cdot CH_3,CF_3CO_2$ and $D\cdot H,CF_3CO_2$. A planar array of O(39), O(40), and C(42) around C(41) is present in each compound.

(4) Noble, M. E.; Huffman, J. C.; Wentworth, R. A. D., *Inorg. Chem.* **1983**, *22*, 1756.
(5) Maatta, E. A.; Wentworth, R. A. D. *Inorg. Chem.* **1979**, *18*, 2409.
(6) Boorman, P. M.; Patel, V. D. *Inorg. Chim. Acta* **1980**, *44*, L85 and references therein.

Table III. Summary of Crystallographic Data

formula	$C_{25}H_{37}F_3Mo_2N_2O_6P_2S_6$
fw	964.76
space group	$A2/a$
a, Å	33.891 (14)
b, Å	16.169 (3)
c, Å	13.902 (3)
β, deg	90.52 (1)
Z	8
V, Å^3	7617.80
density (calcd), g/cm^3	1.682
cryst size, mm	0.10 × 0.10 × 0.10
cryst color	orange
radiation	Mo Kα (λ = 0.710 69 Å) graphite monochromator
linear abs coeff, cm^{-1}	10.94
temp, °C	-165
instrument	Picker 4-circle diffractometer locally modified and interfaced
detector aperture	3.0 mm wide × 4.0 mm high 22.5 cm from cryst
sample to source distance, cm	23.5
takeoff angle, deg	2.0
scan speed, deg/min	4.0
scan width, deg	1.4 + 0.692 tan θ
bkgd counts, s	4 at each end of scan
2θ range, deg	6–50
data collected	11 255 total
unique data	6750
unique data with $F_o > 3\sigma(F_o)$	5400
no. of variables	521
$R(F)$	0.043
$R_w(F)$	0.043
goodness of fit	1.004
largest Δ/σ	0.05

Unlike **D**·H,CF_3CO_2, however, rotational disorder of the CF_3 group does not occur in the methylated derivative.

The alignment of two of the hydrogen atoms of the methanethiolate ligand with the oxygen atoms of the carboxylate ligand can also be seen in Figure 1. This phenomenon appears to be a fortuitous result of molecular packing rather than an indication of significant bonding interactions. The average distance separating these atoms is 2.7 (1) Å, which is approximately the sum of the van der Waals radii. The methyl group appears to be forced into this position by two intermolecular contacts which occur with distances that are also the approximate sum of the appropriate nonbonding radii.

If **D**·H,CF_3CO_2 and **D**·$CF_3CO_2^-$ resemble a thiol and a thiolate of moderate reactivity, they should be incapable of reacting with an unactivated alkene but capable of reacting with an activated alkene. An attempt to prepare the ethyl derivative by the addition of ethylene to **D**·H,CF_3CO_2 failed even after the addition of the tertiary amine. Since the reaction also failed with acrylonitrile, the nucleophilicities of **D**·H,CF_3CO_2 and its conjugate base appear to be less than those of common thiols and thiolates. The behavior of $[(\eta^5\text{-}C_5H_4CH_3)Mo(\mu\text{-}S)(\mu\text{-}SH)]_2$, which remains unique and intriguing, clearly requires further study.

Experimental Section

$[Mo(NC_6H_4CH_3)(S_2P(OC_2H_5)_2)]_2(\mu\text{-}S)(\mu\text{-}SCH_3)(\mu\text{-}O_2CCF_3)$ (D·CH_3,CF_3CO_2). A flask containing $[Mo(NC_6H_4CH_3)(\mu_3\text{-}S)(S_2P(OC_2H_5)_2)]_4$ (0.256 mmol), CF_3CO_2H (2.0 mmol), $(C_2H_5)_3N$ (2.0 mmol), and benzene (5–10 mL) under a blanket of N_2 was charged with an excess of CH_3Br gas, which caused the rapid deposition of $[(C_2H_5)_3NH]Br$. After it was stirred for 2 h, the slurry was filtered in air and the orange filtrate was evaporated to dryness under reduced pressure. Methyl alcohol (10 mL) was added. After the mixture was chilled, the product was collected, washed with cold methyl alcohol, and dried. Recrystallization from a cold mixture of CH_2Cl_2 and CH_3OH afforded orange crystals (87%). Anal. Calcd: C, 31.1; H, 3.9; N, 2.9; S, 19.9. Found: C, 31.8; H, 4.2; N, 3.1; S, 20.1. Selected IR bands (cm^{-1}, KBr): 1650 (s) and 1465 (m) (ν_{CO}), 1205 (vs) and 1158 (m) (ν_{CF}), and 633 (m) (ν_{PS}). ^{1}H NMR (ppm, $CDCl_3$): 1.24, 1.29 (12 H, t, CH_3); 2.08*, 2.16 (6 H, s, arylimido CH_3); 2.27*, 3.08

Table IV. Fractional Coordinates for $[Mo(NC_6H_4CH_3)(S_2P(OC_2H_5)_2)]_2(\mu\text{-}S)(\mu\text{-}SCH_3)(\mu\text{-}O_2CCF_3)$[a]

atom	x	y	z
Mo(1)	1133.9 (1)	634.1 (3)	926.9 (3)
Mo(2)	1508.6 (1)	1599.1 (3)	2380.6 (3)
S(3)	1765.6 (4)	323 (1)	1697 (1)
S(4)	907.5 (4)	1882 (1)	1587 (1)
S(5)	597.6 (4)	885 (1)	−304 (1)
S(6)	1328.3 (4)	−355 (1)	−393 (1)
P(7)	857.9 (4)	38 (1)	−1134 (1)
O(8)	954 (1)	377 (2)	−2172 (3)
C(9)	1211 (2)	1101 (4)	−2291 (4)
C(10)	1621 (4)	788 (9)	−2666 (10)
C(10)′	1155 (4)	1393 (10)	−3242 (11)
O(11)	578 (1)	−675 (2)	−1484 (3)
C(12)	438 (2)	−1321 (4)	−838 (4)
C(13)	219 (2)	−1938 (4)	−1455 (4)
N(14)	884 (1)	−64 (3)	1631 (3)
C(15)	660 (2)	−597 (3)	2193 (4)
C(16)	251 (2)	−483 (4)	2227 (4)
C(17)	26 (2)	−997 (4)	2792 (4)
C(18)	196 (2)	−1633 (4)	3334 (4)
C(19)	600 (2)	−1732 (4)	3294 (4)
C(20)	834 (2)	−1223 (4)	2729 (4)
C(21)	−58 (2)	−2189 (4)	3935 (5)
S(22)	2193.9 (4)	1912 (1)	3056 (1)
S(23)	1419.6 (4)	3041 (1)	2978 (1)
P(24)	1979.2 (4)	3013 (1)	3447 (1)
O(25)	2034 (1)	3184 (3)	4551 (3)
C(26)	1868 (3)	2617 (5)	5246 (5)
C(27)	1819 (3)	3067 (5)	6181 (5)
O(28)	2230 (1)	3771 (3)	3070 (4)
C(29)	2265 (3)	3890 (5)	2012 (6)
C(30)	2483 (4)	4554 (7)	1673 (8)
C(30)′	2152 (6)	4750 (12)	1919 (13)
N(31)	1332 (1)	1055 (3)	3356 (3)
C(32)	1148 (2)	588 (4)	4057 (4)
C(33)	758 (2)	751 (4)	4274 (4)
C(34)	568 (2)	262 (4)	4937 (5)
C(35)	758 (2)	−388 (4)	5400 (4)
C(36)	1153 (2)	−537 (4)	5193 (4)
C(37)	1345 (2)	−45 (4)	4531 (4)
C(38)	542 (2)	−939 (4)	6099 (4)
O(39)	1786 (1)	2235 (2)	1096 (2)
O(40)	1488 (1)	1477 (2)	−53 (3)
C(41)	1697 (2)	2060 (3)	255 (4)
C(42)	1882 (2)	2598 (4)	−534 (4)
F(43)	2029 (1)	3307 (2)	−202 (3)
F(44)	1620 (1)	2798 (3)	−1214 (3)
F(45)	2176 (1)	2196 (3)	−961 (3)
C(46)	2181 (2)	461 (4)	894 (4)
H(1)	67 (2)	−156 (4)	−49 (4)
H(2)	27 (2)	−107 (3)	−30 (4)
H(3)	2 (2)	−169 (4)	−176 (5)
H(4)	41 (2)	−213 (5)	−187 (5)
H(5)	11 (2)	−235 (3)	−109 (4)
H(6)	15 (2)	−12 (4)	184 (4)
H(7)	−23 (2)	−92 (3)	284 (4)
H(8)	69 (2)	−215 (4)	363 (4)
H(9)	110 (2)	−133 (4)	269 (4)
H(10)	−20 (2)	−187 (5)	443 (5)
H(11)	−24 (3)	−251 (6)	361 (6)
H(12)	8 (3)	−255 (5)	430 (6)
H(13)	161 (2)	250 (4)	505 (4)
H(14)	206 (3)	220 (6)	527 (6)
H(15)	202 (3)	323 (6)	640 (6)
H(16)	158 (3)	346 (6)	619 (6)
H(17)	172 (3)	269 (6)	666 (6)
H(18)	62 (2)	110 (4)	393 (4)
H(19)	32 (2)	36 (4)	509 (4)
H(20)	127 (2)	−94 (4)	549 (5)
H(21)	162 (1)	−14 (3)	439 (4)
H(22)	64 (3)	−89 (6)	663 (7)
H(23)	23 (3)	−86 (6)	612 (7)
H(24)	51 (4)	−144 (7)	572 (8)
H(25)	237 (2)	6 (5)	108 (6)
H(26)	209 (2)	46 (4)	30 (5)
H(27)	233 (2)	95 (4)	100 (4)

[a] Fractional coordinates are ×10^4 for non-hydrogen atoms and ×10^3 for hydrogen atoms.

(3 H, s, bridging SCH_3); 4.12 (8 H, m, CH_2); 6.65*, 6.67 (8 H, q, arylimido H). ^{31}P NMR (ppm, $CDCl_3$): 114.3*, 114.5. In each NMR spectrum, the chemical shifts of the major conformer, where distinguishable from the minor conformer, are designated with an asterisk.

$[Mo(NC_6H_4CH_3)(S_2P(OC_2H_5)_2)]_2(\mu\text{-}S)(\mu\text{-}SC_2H_5)(\mu\text{-}O_2CCF_3)$. A similar procedure was used except that the quantity of C_2H_5Br was equivalent to that of the carboxylic acid (2.0 mmol) and the reaction was conducted for 3 h under an atmosphere of N_2 on a steam bath. After recrystallization, the yield of orange crystals was 78%. Anal. Calcd: C, 31.9; H, 4.0. Found: C, 31.8; H, 4.2. Selected IR bands (cm^{-1}, KBr): 1643 (s) and 1464 (m) (ν_{CO}), 1202 (vs) and 1154 (m) (ν_{CF}), and 634 (m) (ν_{PS}). ^1H NMR (ppm, $CDCl_3$): 1.25 (12 H, m, CH_3); 1.80*, 1.92 (3 H, t, CH_3 of bridging SCH_2CH_3); 2.10*, 2.15 (6 H, s, arylimido CH_3); 2.38*, 3.34 (2 H, q, CH_2 of bridging SCH_2CH_3); 4.13 (8 H, m, CH_2); 6.56*, 6.65 (8 H, q, arylimido H). ^{31}P NMR (ppm, $CDCl_3$): 114.2, 114.4*. Conformer ratio: 1.3 at about 20 °C. Coalescence temperature: about 44 °C.

$[Mo(NC_6H_4CH_3)(S_2P(OC_2H_5)_2)]_2(\mu\text{-}S)(\mu\text{-}SCH_2C_6H_5)(\mu\text{-}O_2CCF_3)$. Again, a procedure similar to that employed with the methyl derivative was used except that the quantity of $C_6H_5CH_2Br$ was equivalent to that of the carboxylic acid (2.0 mmol). The yield of orange crystals after recrystallization was 73%. Anal. Calcd: C, 35.8; H, 4.0. Found: C, 35.7; H, 4.1. Selected IR bands (cm^{-1}, KBr): 1642 (s) and 1464 (m) (ν_{CO}), 1203 (vs) and 1158 (s) (ν_{CF}), and 651 (m) and 636 (m) (ν_{PS}). ^1H NMR (ppm, $CDCl_3$): 1.24, 1.32 (12 H, t, CH_3); 2.05*, 2.17 (6 H, s, arylimido CH_3); 3.44*, 4.53 (2 H, s, CH_2 of bridging $SCH_2C_6H_5$); 4.15 (8 H, m, CH_2); 6.50*, 6.70 (8 H, q, arylimido H); 7.4–7.8 (5 H, m, aryl H of bridging $SCH_2C_6H_5$). ^{31}P NMR (ppm, $CDCl_3$): 114.0*, 114.2. Conformer ratio: 5.5 at about 20 °C. Coalescence temperature: about 38 °C.

X-ray Crystallography. Cell dimensions, some of the details for the collection of data, and final residuals are given in Table III while the methods used for the solution and refinement of the structure are available as supplementary material. Positional parameters for all atoms can be found in Table IV.

Acknowledgment. Support for this research was provided by USDA Grant No. 59-2184-0-1-434-0. The authors also acknowledge support from the Bloomington Academic Computing Service for use of the computing facilities.

Registry No. **D**·H,CF_3CO_2, 88548-67-8; **D**·CH_3,CF_3CO_2, 88548-64-5; **D**·C_2H_5,CF_3CO_2, 88548-65-6; **D**·$CH_2C_6H_5,CF_3CO_2$, 88548-66-7; $[Mo(NC_6H_4CH_3)(\mu_3\text{-}S)(S_2P(OC_2H_5)_2)]_4$, 73037-71-5.

Supplementary Material Available: Details of solution and refinement of the structure and listings of anisotropic thermal parameters, all bond distances and angles, and observed and calculated structure amplitudes (52 pages). Ordering information is given on any current masthead page.

Additions and Corrections

1983, Volume 22

Melvin L. Morris and R. D. Koob*: Mass Spectra of Rhodium(III) and Ruthenium(III) Complexes of 2,4-Pentanedione, 1,1,1-Trifluoro-2,4-pentanedione, and 1,1,1,5,5,5-Hexafluoro-2,4-pentanedione.

Page 3502. An error appeared in the title of this paper. The correct version is that printed here.—R. D. Koob